FORTY-FOURTH ANNUAL SYMPOSIUM ON FREQUENCY CONTROL

A RUBIDIUM FREQUENCY STANDARD AND A GPS RECEIVER: A REMOTELY STEERED CLOCK SYSTEM WITH GOOD SHORT-TERM AND LONG-TERM STABILITY

by

David W. Allan and Judah Levine
Time and Frequency Division
National Institute of Standards and Technology
Boulder, CO 80303

Abstract

The short-term stability of a rubidium gas-cell frequency standard is usually better than that of commercial cesium-beam frequency standards. In the short-term stability region (from a few seconds to several thousand seconds) and for the specific value $\sigma_y(\tau = 100\ s)$, the range of short-term stabilities for rubidium is from about 4 to 10 x 10^{-13}, and for cesium about 6 to 30 x 10^{-13}. In the short-term, the stability improvement for rubidium and cesium is proportional to $\tau^{-1/2}$. Cesium almost always has better stability in the long-term because cesium has less sensitivity to environmental perturbations. For example, cesium has little or no frequency drift, whereas rubidium usually does. Improving a clock's environment invariably improves the long-term performance, especially in the case of rubidium.

Satellite time transfer shows a day-to-day stability of about a nanosecond. The spectrum of the fluctuations implies that $\sigma_y(\tau)$ should decrease as τ^{-1}. If a rubidium standard, in a good environment with the above performance in the short-term, were married to a satellite time-transfer system, then the combined performance of the system could have better short-term and better long-term stability than a stand-alone, free-running, commercial cesium standard.

We have taken some data to test this idea. The conclusions confirm the hypothesis. We have also replaced the rubidium oscillator with a quartz oscillator and with a high-performance commercial cesium standard. In both cases the system had significantly improved long-term stability over what otherwise would be obtainable from either oscillator by itself.

Introduction

Most commercial rubidium frequency standards have better short-term frequency stability than commercial cesium-beam frequency standards, where short-term implies averaging times (τ) up to a few thousand seconds. Placing a rubidium standard in a good environment usually extends its short-term stability to longer τ values (of the order of a day). For τ longer than a day, the opposite is most often true; that is, cesium is better than rubidium in the long-term.

The measurement noise of transferring time and frequency to a remote location using the Global Positioning System (GPS) common-view (C-V) technique can reach $\sigma_y(\tau = 1\ day)$ values approaching 1×10^{-14}, where $\sigma_y(\tau)$ is the square-root of the two-sample or Allan variance.[1] Therefore, an environmentally controlled rubidium standard, together with a GPS time transfer receiver, has the potential for the following advantages (taken as a system):

1) For a lesser cost, both the short and the long-term stability can be better than that of a commercial cesium standard;
2) in the long-term the system can reflect the stabilities of some of the best time and frequency standards in the world, in that it can be both syntonized and synchronized to a primary reference;
3) the system can be made fully automatic;
4) the system can remove the usual frequency accuracy limitation of rubidium including the frequency drift--allowing the system to be as accurate as the reference standard; and
5) the system can remove the usual time accuracy limitation of either cesium or rubidium--allowing the system to be synchronized to within a few nanoseconds of the reference standard.

Some of the disadvantages are:

1) The system's feedback is by a daily telephone call between the system and the reference standard used in the GPS common-view (GPS C-V) mode; and
2) the rubidium standard needs a good

Contribution of the U.S. Government, not subject to copyright.

environment to achieve the desired intermediate stability goals.

Figure 1 is a sketch of the GPS-common-view, remote-clock servo concept. Figure 2 shows some more detail for the remote clock at site B. We assume that the clock at site A has good long-term stability. One of our goals is to transfer the long-term stability of clock A to the clock at site B with the time transfer capability of GPS C-V. The theory we used for designing a digital servo for this system is based on a thesis of Alain Guetrot [2]. The essential concept of his thesis is that if the measurement noise spectrum, $S_N(f)$, can be represented as

$$S_N(f) \sim f^{\beta}$$

and the signal spectrum, $S_S(f)$, as

$$S_S(f) \sim f^{\beta-2},$$

then an exponential filter is optimum for obtaining the best signal-to-noise ratio. Here β is typically an integer between 3 and -5. What is measured, of course, is signal plus noise. If the measurements are a discret time series then a practicle realization of an exponential filter is the following,

$$z_i = \frac{kz_{i-1} + \hat{z}_i}{k+1}, \qquad (1)$$

where k is proportional to the exponential filter time constant, z_{i-1} is the last best estimate, $\hat{z}_i$ is the current measurement (signal plus noise) and z_i is the current best estimate of the signal, that is, the true difference of clock A compared to B.

We assume flicker noise time or phase modulation (PM) for the measurement noise (GPS C-V) and flicker noise frequency modulation (FM) for the long-term stability of the remote clock. This model, which satisfies the assumption in Guetrot's analysis, was tested and was found to be reasonable for the set of common-view data we analyzed and for the kinds of clocks we may use at A and/or B (quartz, rubidium, cesium and/or hydrogen frequency standards) for selected regions of sample times, τ, as determined from a $\sigma_y(\tau)$ diagram.

We assume clock B has frequency drift, so that the time prediction equation can be written as

$$\hat{x}(t) = x(t-\tau) + y(t-\tau) \cdot \tau + \tfrac{1}{2}D(t-\tau) \cdot \tau^2, \qquad (2)$$

where $x(t-\tau)$, $y(t-\tau)$ and $D(t-\tau)$ are the best estimates of

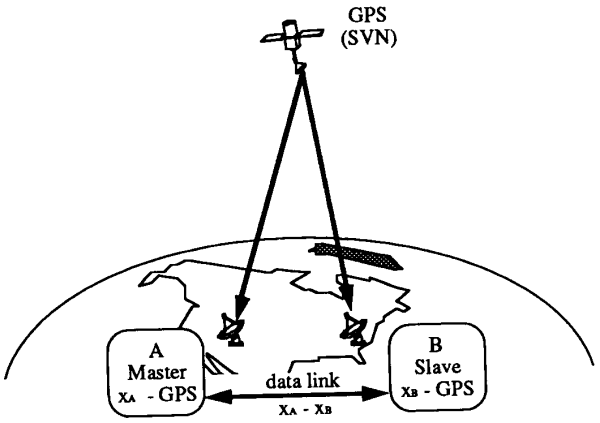

Figure 1. A schematic diagram showing how to provide accurate and stable time and frequency at a remote site. If the clock at site B is a rubidium gas-cell frequency standard in a good environment, and given the levels of GPS common-view measurement noise, the net output can be that time and frequency at the remote site is better in long-term as well as in short-term than that from a commercial cesium standard by itself.

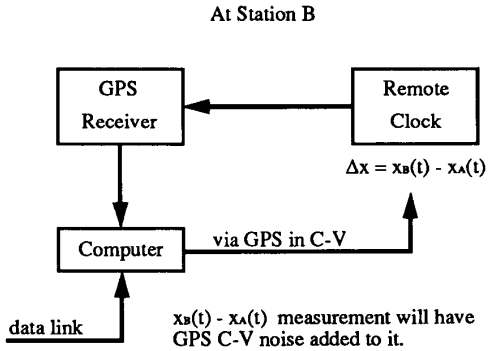

Figure 2. A block diagram of the GPS common-view time transfer receiver combined with a clock at site B. The system achieves better short-term and long-term, time-and-frequency stability than would be available from a commercial cesium standard by itself.

the time offset, the normalized frequency offset and the normalized frequency drift of the remote clock at the last measurement, and τ is the prediction interval. In our case, the prediction interval was usually one sidereal day - using a single satellite in the GPS C-V mode. For a general prediction interval $\tau = n\tau_0$, where τ_0 = 1 sidereal day, we may write the best estimate of the exponential time difference as

$$x(t) = (k_x\hat{x}(t) + n\,\Delta x)/(k_x + n), \quad (3)$$

where k_x is proportional to the exponential filter time constant for the best time difference estimate. n gives more weight to the measurement to compensate for flicker FM in the clock where the rms time error of prediction is proportional to n, and Δx is the measured common-view time difference between clock B and clock A. The exponential filtered drift is

$$D(t) = [k_D D(t-\tau) + \hat{D}]/(k_D + 1), \quad (4)$$

where $\hat{D}$ is the drift estimated over the last two measurement intervals, and is given by

$$\hat{D} = \frac{\dfrac{x(t) - x(t-\tau)}{\tau} - \dfrac{x(t-\tau) - x(t-\tau-\tau_{-1})}{\tau_{-1}}}{\dfrac{\tau + \tau_{-1}}{2}}, \quad (5)$$

where τ_{-1} is the measurement interval before the last one. The normalized frequency offset estimate is given by

$$y(t) = \{k_y[y(t-\tau) + D(t)\cdot\tau] + \hat{y}(t)\}/(k_y + 1), \quad (6)$$

where k_y is proportional to the exponential filter time constant for the best normalized frequency offset estimate, and

$$\hat{y}(t) = \frac{x(t) - x(t-\tau)}{\tau} + \tfrac{1}{2}D(t)\cdot\tau. \quad (7)$$

The k_x, k_y and k_D parameters are functions of τ_0, the measurement noise type and level and the noise type and level of the clocks at A and B. The parameters can be optimized through simulation or with real data. We used the latter. The above recursive equations assume τ is the time since the last measurement. The measurement intervals need not be equal.

Experimental Results

The rubidium frequency standard used for the experiment was an engineering development model for the GPS program. It was placed in vacuum with a temperature controlled environment so that variations were less than 0.1°C. The quartz oscillator frequency standard was a special one designed for short-term and long-term stability. It was also placed in a special environment [3].

A plot of the free-running fractional frequency of the rubidium is shown in Figure 3a and its frequency stability is plotted in Figure 3b. If a frequency drift is subtracted, the spectrum for the long-term stability is reasonably modeled by flicker FM. Figure 4 shows a plot of the frequency stability of the quartz oscillator. A frequency drift has been subtracted from the quartz data before plotting the stability. The nominal τ^0 behavior corresponding to flicker FM is apparent. The frequency stability of the GPS C-V measurement noise is plotted in Figure 5, and the τ^{-1} behavior is indicitive of flicker noise PM. Hence, we see that the assumptions needed for the Guetrot thesis are satisfied.

The two GPS receivers were colocated for convenience in checking the truth of the hypothesis. Colocating the receivers will cause a cancellation of the broadcast ephemeris errors, ionospheric delay errors and tropospheric delay errors as well. Errors due to multipath effects and to the receivers will remain about the same for long-baseline separations between the clocks. Therefore, the experimental results obtained in this paper may tend to give better stabilities than would be obtained where there is a large distance between clocks A and B. However, similar levels of GPS C-V measurement noise are often achieved over long baselines if several satellites are used and the data are properly combined, weighted and filtered [1,4].

Figures 6 and 7 are plots of the predicted values minus the measured values ($\hat{x}(t) - \Delta x$) for rubidium and the quartz, respectively, using the GPS C-V servo illustrated in Figures 1 and 2. The errors between the times of the measurements will usually be smaller than the errors plotted. There was a several day break in the continuity of the data between MJD 47615 and 47621 as can be seen in Figures 6 and 7. Before this break, there were a few days for the servo parameters to initialize. This initialization allowed for a reasonable prediction across this break in

data continuity. We can learn two important things from this fortuitous break in data continuity. First, we can see the ability of the system to predict time over several days; and second, we can see the transient response of the system as it re-acquires the daily signal.

Figures 8 and 9 are plots of the frequency stabilities of the errors plotted in Figures 6 and 7 for rubidium and quartz, respectively. We see that after only a few days of integration, this system has the capacity to track the best primary frequency standards in the world.

Figures 10 and 11 are the corresponding time stability plots where the time stability, $\sigma_x(\tau)$, is defined as $\tau * \mathrm{mod}\sigma_y(\tau)/\sqrt{3}$. [5,6] For rubidium (Figure 10) the system stability for single one-day measurements is within 10 ns (rms) of clock A. And again, for times between the measurement times, the stabilities will usually be less than this number. If we average the time readings for a few days, we can approach a nanosecond of time stability. The average value for the data in Figure 6 is 0.05 ns. There will typically be biases of a few nanoseconds in the GPS C-V measurement technique; hence, the time accuracy cannot be better than these biases.

The corresponding single one-day measurement stability number for the quartz oscillator stability plotted in Figure 11 is 75 ns (rms). We see, in this case, that we have to average for very long periods to approach a time stability level of 1 ns. That one can reach these levels at all with a quartz oscillator in the system is impressive. The mean value for the time errors plotted in Figure 7 was 0.5 ns. Again, please note that biases in the system will limit the time accuracy to a few nanoseconds.

We tested the system with a high-performance, commercial, cesium-beam frequency standard as the clock at site B and observed long-term improvements. The improvements were not nearly so dramatic as for the above data for rubidium and quartz. The main benefits for using cesium in the system is to keep the time at site B synchronized. The cost effectiveness for such a system is obviously better with rubidium and quartz kept in a good environment.

Methods of Implementation

This servo could be implemented in several different ways. The outputs of the model could be used as a "paper" time or frequency output. This is simple to implement but has the disadvantage that electrical output of the oscillator does not directly reflect the improvement in performance produced by the servo. This disadvantage may be overcome by using the model parameters to drive a microstepper or other similar device to produce a continuously corrected output. A small computer would be required to control the microstepper and to cope with missing data.

Another novel alternative is to provide an input to the system from an unknown clock a user may wish to calibrate. The system would measure the time and frequency difference between the clock being calibrated and the clock, which is part of the system at B. The system, at anytime, has the information for the best estimate of the time and frequency difference between clocks A and B. Hence, the system could straight forwardly calculate the optimum estimate of the clock being calibrated against the reference clock at site A. This information could be provided as a real-time read out of the system and would be more precise and accurate than that obtainable from a steared micro-phase stepper.

The designer can vary parameters k_x, k_y and k_D so as to optimize the transient response of the servo or its rms offset error (but not both simultaneously). Likewise, the threshold for rejecting a measurement must be chosen as a compromise between detecting time or frequency steps and providing immunity to glitches.

The values of the parameters chosen for the data presented in this paper were $k_x = 25$, $k_y = 1$ and $k_D = 0.2$ for rubidium and $k_x = 20$, $k_y = 0$ and $k_D = 0.2$ for quartz. These values were chosen to obtain a best transcient response rather than optimizing steady-state stability. From the results obtained, this choice caused little degradation in the steady-state performance.

The time transfer system need not be the GPS C-V method. Any system, which would allow the time difference comparison of clocks remote from each other at the few nanoseconds level, could be made to provide comparable results as those reported in this paper. In addition, the performance of the system when using GPS C-V is unaffected by GPS selective availability (SA) if only clock dither is turned on (no degradation of the satellite broadcast ephemeris). If, however, GPS SA were fully implemented, including the degradation of the broadcast satellite ephemeris, then some of this degradation would not be canceled in the GPS C-V approach. The amount of increased measurement noise is a function of the baseline between the clocks and the level of SA.

We are currently studying more complex algorithms in which the k_x, k_y and k_D parameters are adjusted dynamically in response to changing conditions.

Acknowledgements

The authors wish to thank Dr. Donald B. Sullivan, Dr. Marc Weiss and Mr. Tom Weissert for helpful suggestions on the manuscript. We are especially grateful to the sponsors: the Joint Program Office of Air Force Space Division and the Naval Research Laboratory for supplying the rubidium clock.

References

[1] M. A. Weiss and D. W. Allan, "An NBS Calibration Procedure for Providing Time and Frequency at a Remote Site by Weighting and Smoothing of GPS Common View Data," IEEE Trans. on Instrum. and Meas., IM-36, 572-578 (1987).

[2] A. G. Guétrot, "Optimum Smoothing Techniques on VLF Time Signals," Thesis, University of Colorado, 1969.

[3] F. L. Walls, "Environmental Effects on the Medium and Long Term Frequency Stability of Quartz Oscillators, Proc. of the 2nd European Frequency and Time Forum, Neuchatel, Switzerland, March 16-17, 1989, pp. 719-727.

[4] M. A. Weiss, "The Design of Kalman Smoothers for Global Positioning System Data," IEEE Trans. and Meas., 38, 652-657 (1989).

[5] D. W. Allan, "Time and Frequency (Time-Domain) Characterization, Estimation, and Prediction of Precision Clocks and Oscillators," IEEE Transactions on Ultrasonics, Ferroelectrics, and Frequency Control, UFFC-34, 647-654 (1987).

[6] D. W. Allan, D. D. Davis, J. Levine, M. A. Weiss, N. Hironaka, and D. Okayama, "New Inexpensive Frequency Calibration Service from NIST," these proceedings.

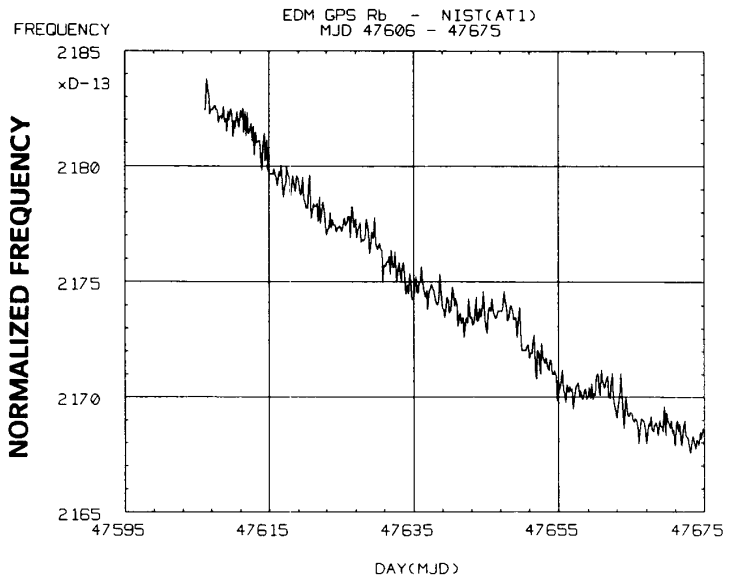

Figure 3a. A plot of the normalized frequency output of an engineering-development-model, rubidium-gas-cell frequency standard. This EDM standard was prepared as part of a GPS program.

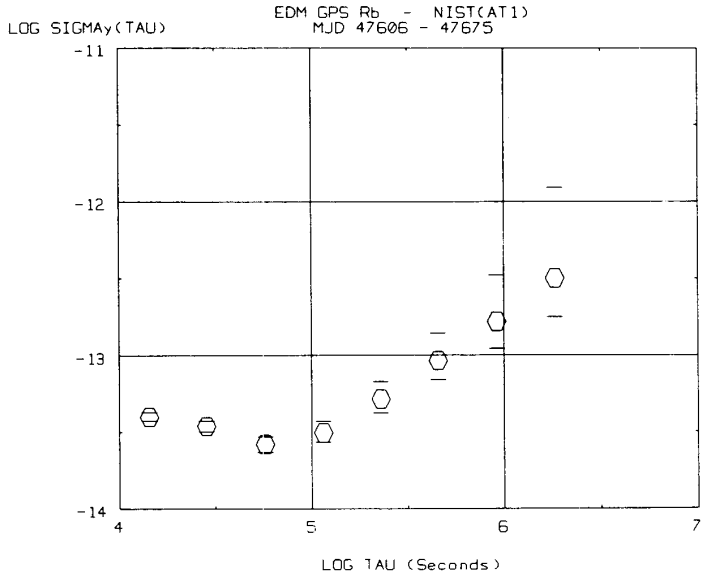

3b. A plot of the frequency stability of the data plotted in Figure 3a with no frequency drift removed. The long-term stability is limited by the drift: $\sigma_y(\tau) = \tau D/\sqrt{2}$.

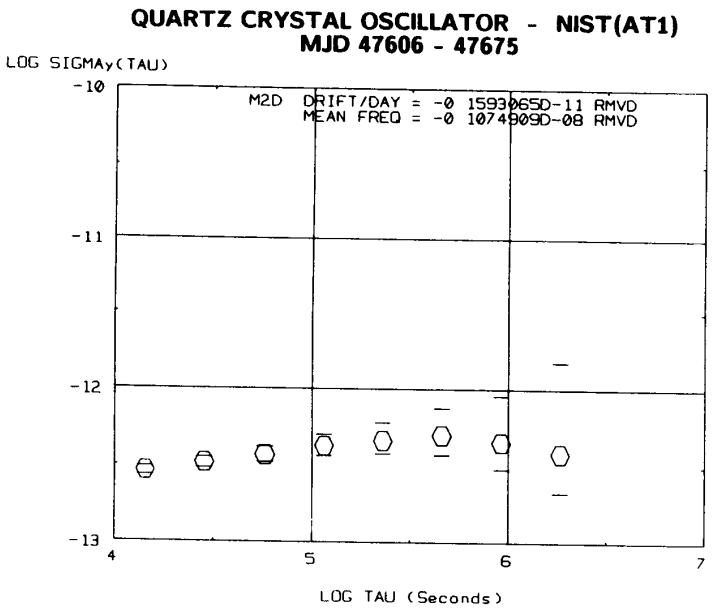

Figure 4. A plot of frequency stability for a special quartz oscillator frequency standard placed in a good environment. A frequency drift was subtracted from the data before calculating the frequency stability as plotted.

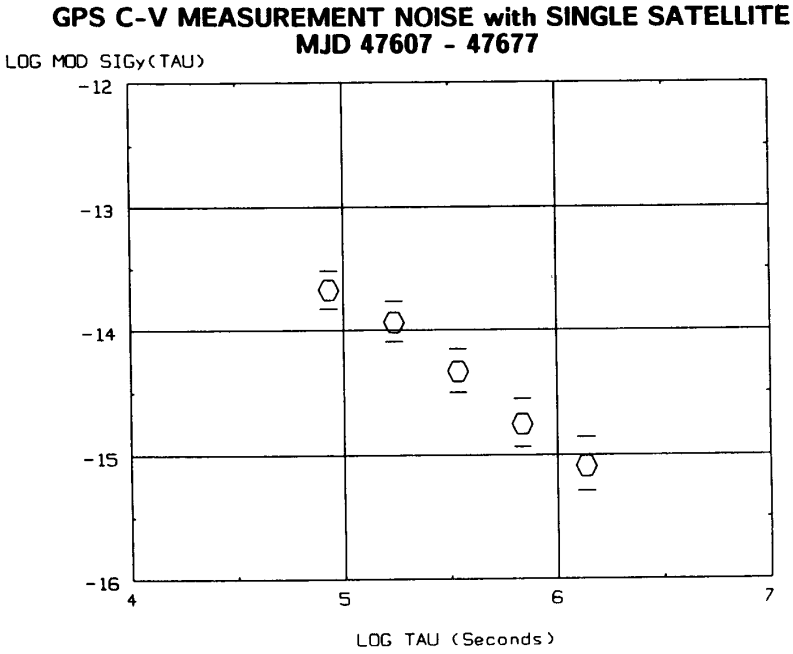

Figure 5. The frequency stability measurement noise for the GPS common-view system used for providing time and frequency at a remote site.

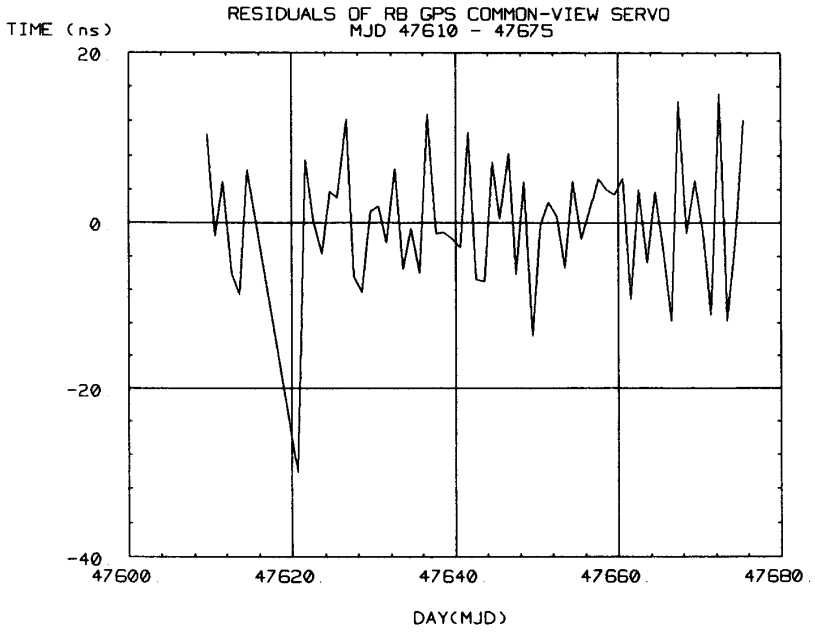

Figure 6. A plot of the predicted time values minus the measured values for a rubidium-gas-cell frequency standard in a good environment at site B.

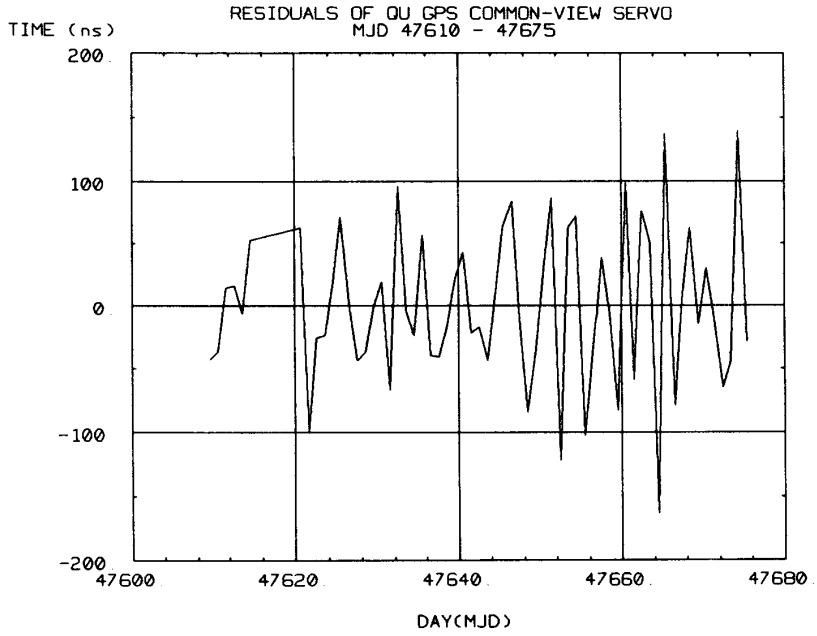

Figure 7. A plot of the predicted time values minus the measured values for a quartz-crystal oscillator in a good environment at site B.

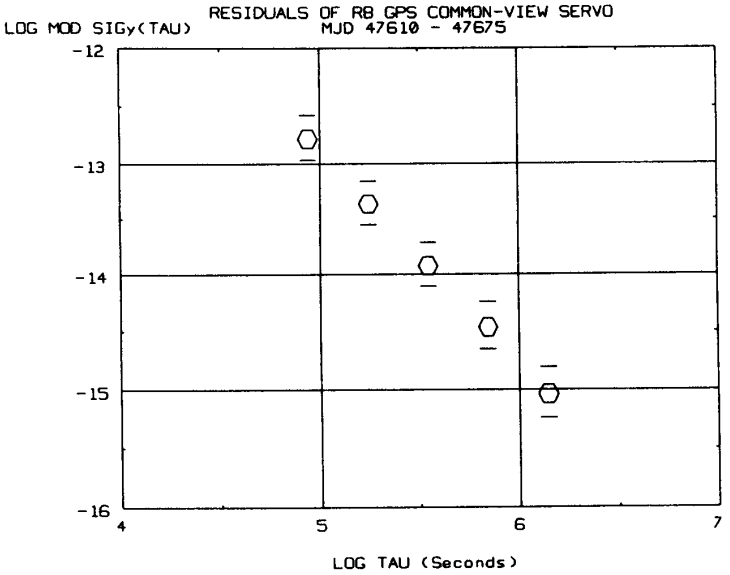

Figure 8. A plot of the frequency stability of the errors plotted in Figure 6.

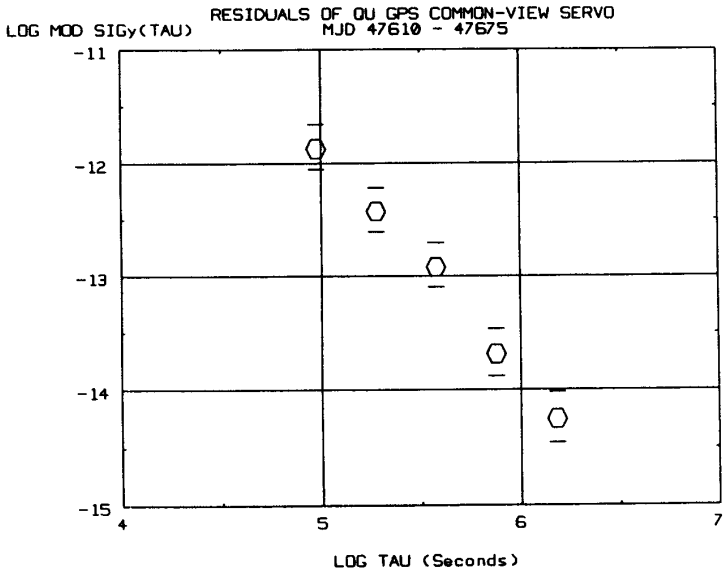

Figure 9. A plot of the frequency stability of the errors plotted in Figure 7.

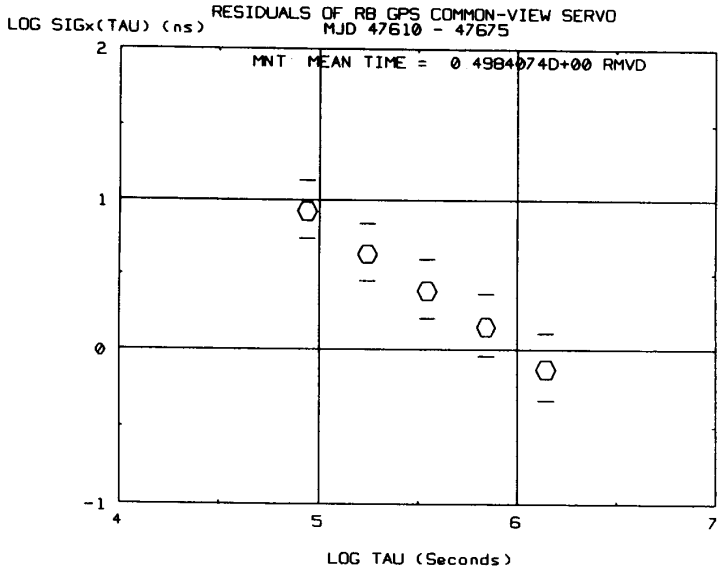

Figure 10. A plot of the time stability of the errors plotted in Figure 6.

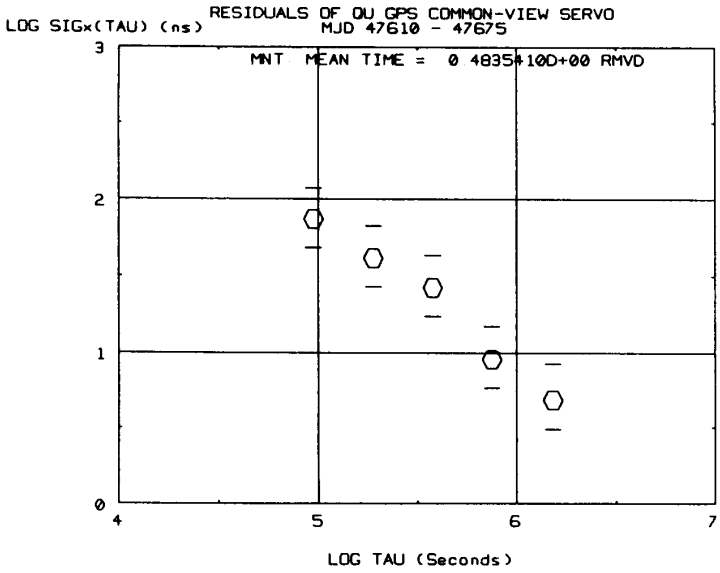

Figure 11. A plot of the time stability of the errors plotted in Figure 7.